ISSN 1063-7826, Semiconductors, 2020, Vol. 54, No. 14, pp. 1873–1876. © Pleiades Publishing, Ltd., 2020.

NANOSTRUCTURES AND LIFE SCIENCES

A Single-Molecule Label-Free Identification of Single-Nucleotide Colorectal-Cancer-DNA Polymorphism Using Impedance Spectroscopy of Self-Redox-Active Decorated Carbon Nanotubes

V. P. Egorova[a], H. V. Grushevskaya[b,*], A. S. Babenka[c], R. F. Chakukov[b], N. G. Krylova[b,d], I. V. Lipnevich[b], and E. V. Vaskovtsev[a]

[a] *Belarusian State Pedagogical University, Minsk, Belarus*
[b] *Belarusian State University, Minsk, Belarus*
[c] *Belarusian State Medical University, Minsk, Belarus*
[d] *Belarusian State Agrarian Technical University, Minsk, Belarus*
**e-mail: grushevskaja@bsu.by*

Received June 19, 2020; revised June 19, 2020; accepted July 17, 2020

Abstract—A novel label-free impedance assay which is based on self-redox active carbon nanotube arrays decorated by nanocyclic organometallic complex monolayer is offered to discriminate single-nucleotide polymorphism of colorectal-tumor genome. The assay is based on the following effects. A mass transfer for the multiwalled carbon nanotubes (MWCNTs) is testified by a Cole–Cole plot with Warburg impedance in dielectric spectra. Charging $K(K')$-point of graphene Brillouin zone is associated with the mass transfer for MWCNTs that leads to arising of charged MWCNT-end states. Plasma oscillations of charge carriers shield electric field of charged electrodes. Complementary hybridization of target deoxyribonucleic acid (DNA) with probe DNA on the MWCNT surface facilitates the penetration of single-stranded target DNA in the nanopores. Dielectric-band appearance and shielding effects testify the duplex formation.

Keywords: DNA analysis, single nucleotide polymorphism, impedance spectroscopy, carbon nanotubes, Langmuir–Blodgett film

DOI: 10.1134/S1063782620140092

1. INTRODUCTION

Modern methods of molecular-genetic analysis, which are used in clinical practice, require an amplification of target single-stranded (ss) DNA sequences in polymerase chain reaction (PCR). However, the extremely low concentrations of tumor DNA are out of detection limit of PCR-based methods because the losses of the target DNA in the isolation, purification and detection processes. Because of very small concentrations from 0.01 to 0.002% of mutated allele DNA in the cancer samples, only single double-stranded (ds) DNA molecules with single-nucleotide mismatch (gene point-mutation or single nucleotide polymorphism (SNP) of genome) are isolated from tumor tissue of patients at early-stage cancer. Single long DNA molecules in the plasma of patients with cancer are diagnostic marker and prognostic factor also. Because of these facts new methods of DNA-analysis should be developed [1, 2]. The most promising method for sequencing of single DNA molecules in samples is nanosequencing based on surface plasmon resonance effects and surface-enhanced Raman scattering in quantum materials: nanoparticles, graphene, carbon nanotubes, graphene-like monomolecular layers (monolayers) and nanostructured composite materials [3, 4]. In the present work we utilize long ds- and short ss-DNA-probes for label-free genotyping. The purpose of this study is to perform dielectric and Raman spectral analysis of DNA-hybridization on surface of decorated-MWCNT monolayer suspended on nanopores and to develop an label-free impedance assay utilizing self-redox activity of carboxylated MWCNTs decorated by nanocyclic organometallic complexes to discriminate single-nucleotide polymorphism of colorectal tumor genome.

2. EXPERIMENTAL

2.1. Materials

We utilize two types of DNA probes at single-base-mismatch discrimination: short primer ss-DNAs for perfect-matched (wild-type) and single-mismatched (mutant-type) hybridization with native ds-DNAs and long primer single-base mismatched ss-DNA/blocker

Table 1. Oligonucleotide sequences used in experiments

Oligonucleotide name	Sequence structure (5' → 3')
wild-type ss-DNA probe $KRAS_w$	GTTGGAGCTGGTGGCGTAG
mutant-type ss-DNA probe $KRAS_m$	AGTTGGAGCTGATGGCGTAG
long primer single-base mismatched ss-DNA_{lp}	ATAAGGAGGCACTCTTGCCTACGCCATCAGCTCCAACTACCA-CAAG
blocker ss-DNA_{W_m}	TTGTGITAGTTGGAGCTGATGICGTAGICAAIAGTICCT
target single-base mismatched ss-DNA_{lm}	CTTGTGGTAGTTGGAGCTGATGGCGTAGGCAAGAGTG-CCTCCTTATT

composition system as ds-DNA probe for complementary hybridization with a mutant-type oligonucleotide sequence ss-DNA_m. The blocker oligonucleotide prevents a hairpin-structure formation and contains inosine (I) substitutions. All oligonucleotide label-free probes are presented in Table 1. The DNA probes were purchased in "Primetech ALC" (Minsk, Belarus). An oncogene KRAS, native ds-DNA_T isolated from colon-cancer tumor, and placental ds-DNA_P of healthy donors were utilized as a marker gene. The purity of the DNA samples was confirmed by a spectrophotometric method. All experiments were performed at room temperature. For experiment, the ds-DNA probe was prepared by annealing at 2:1 ratio of the blocker ss-DNA_{W_m} to ss-DNA_{lp} in TE buffer at 37 ± 0.1°C. The hybridization reaction lasted 30 minutes. All chemical reagents of analytical grade were used without further purification.

Biosensitive nanostructured ultra-thin films which transduce hybridization signals was fabricated by the Langmuir–Blodgett (LB) technique and consisted of five monomolecular layers (monolayers) formed by nanocyclic complexes of high-spin octahedral iron with dithionylpyrrole (DTP) ligands and two monolayers from complexes of carboxylated hydrophilic MWCNTs with different DNA-probes.

2.2. Methods

Electro-physical studies have been performed using planar interdigital electrode structures on pyroceramic support. The dielectric coating of the electrodes represents itself a nanoporous anodic alumina layer (AOA) with a pore diameter of 10 nm. The synthesized LB-nanoheterostructures were suspended on the interdigital electrode system. The fabricated capacitive DNA-nanosensors are sensors of non-Faraday type. To excite harmonic auto-oscillations of electric current (charging–discharging processes in the capacitors), the sensor was connected as the capacitance C into the relaxation resistance (R)—capacitor (C) oscillator (self-excited RC-oscillator).

Spectral studies in visible range were carried out using a confocal micro-Raman spectrometer Nanofinder HE ("LOTIS-TII", Tokyo, Japan-Belarus) by laser excitation at wavelengths 532, 785 nm at room temperature.

All results were confirmed by Sanger sequencing method. We have discriminated mutation and wild type in 100% of 20 samples.

3. RESULTS AND DISCUSSION

3.1. MWCNT-Enhanced Hight Scattering and MWCNT-Based Quenching

Light scattering in aromatic compounds is quenched by π–π-stacking interaction at touching molecular ring planes to MWCNT surface. Pyrrole and thiophene rings in the metal-containing LB-DTP-monolayers are enough distant from surface MWCNT because of that vibrations of these groups do not quench but resonate with collective oscillations of free charge carriers (plasmons) in the nanotubes. Plasmon resonance provides enhancement of light scattering in the DTP-monolayers. It is testified by intensive bands of Raman spectra of DTP (see Fig. 1a).

MWCNT-enhanced long-distance energy transfer is excited in the DTP monolayers with a hybridized ds-DNA at the green laser excitation with 532 nm as Fig. 1a demonstrates. The charge transfer into high excited levels is originated by perfect match between $KRAS_m$ and the mutant ds-DNA_T of colorectal cancer tissue. Chiral massless charge carriers confined on MWCNT surface are in lower impurity levels and become free after excitation of the impurity charge carriers to the high energy levels. Therefore, destroying of electron-hole pairs in graphene plane leads to decreasing number of charged $K(K')$, Γ-points of graphene Brillouin zone for MWCNTs and, accordingly, the intensity of G band of the spectrum in Fig. 1a decreased. Complementary hybridization between the

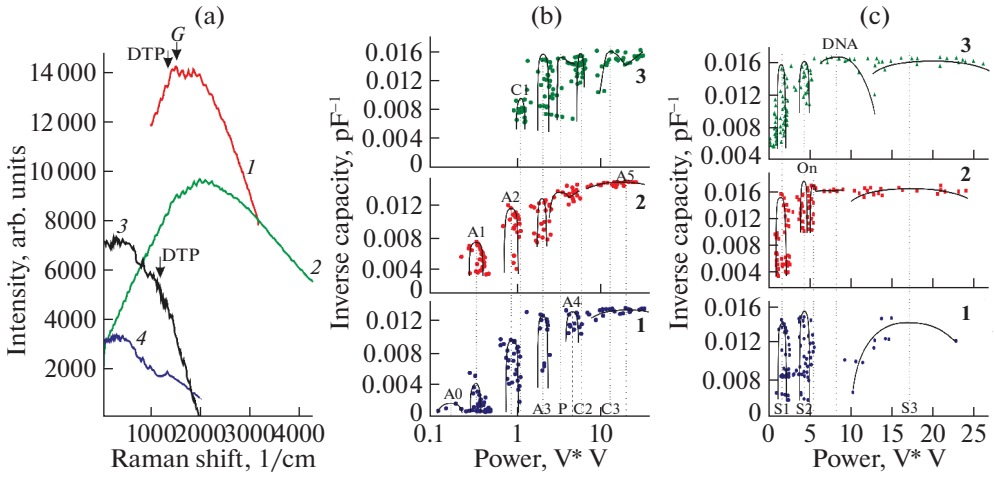

Fig. 1. (a) Raman spectra of decorated MWCNTs after hybridization of target DNA_T with $KRAS_w$ (spectra *1*, *3*) and $KRAS_m$ (spectra *2*, *4*) on MWCNT surface. Wavelengths of laser excitation were 532 (*1*, *2*), 785 nm (*3*, *4*); (b) Dielectric spectra: "1" for nanoporous AOA, "2" for metal-containing DTP-LB-film deposited on AOA, "3" for decorated MWCNTs suspended on nanopores; (c) dielectric spectra: "1" and "2" for DNA-sensor with $KRAS_w$ and a probe system $KRAS_w$–ds-DNA-probe respectively, "3" after bindin with target ss-DNA_{lm}. Cole–Cole plots in the spectra are marked as A*i*, *i* = 0, ..., 5 for AOA; "P" for the DTP compound and C*i*, *i* = 0, ..., 3 for MWCNTs; S*i*, *i* = 0, ..., 3 for DNA-sensor with $KRAS_w$ only; "'On"' for ds-DNA probe; "DNA" for duplex.

single-stranded chain of target ds-DNA_T and the DNA-probe $KRAS_m$ leads to touching between MWCNTs and DTP surfaces because the distortion of ON/MWCNT complexes by formed perfect duplexes. Then the target ss-DNA_T penetrates through nanocavities of nanocyclic compound into the nanopores. As result, Coulomb forces between the DNA and self-redox active DTP-monolayers push out the last from nanopore and, accordingly, the touching surface for DTP-molecules and MWCNTs grows with subsequent increment of π–π-stacking. Meanwhile, a decrement in the impurity energy levels makes them acceptable for MWCNT charge carriers. Since the chiral charge carriers occupy and are not destroyed on the impurity levels the transitions of impurity charges are suppressed in virtue of Pauli exclusion principle signifying that MWCNTs quench scattering light with wavelengths 532, 785 nm in the transducer after the hybridization as comparison between pairs of spectra *1–2* and *3–4* in Fig. 1a shows.

3.2. Impedance Spectroscopy Analysis

Dielectric spectra of studied nanostructures are shown in Figs. 1b, 1c. Opposite to nanoheterostructures, dielectric spectra of nanoporous alumina do not contain dielectric Cole–Cole plots (bands) with diffusion element or Warburg impedance *W*. Since the Warburg impedance is absent for AOA and, accordingly, the oxidation of aluminium electrodes does not occurs, the formed nanoheterostructures are stable. The Cole–Cole plot for the metal-containing dithionylpyrrole LB-films testifies both electric capacity of Helmholtz double layer and the Warburg impedance *W* of diffusion layer in which electrochemical reactions with mass transfer proceed (self-redox activity). The oxidation-reduction potential of dithionylpyrrole films emerges due to self-redox activity of pyrrole groups with transport of electric charge along conjugated double bonds. MWCNTs are also self-redox active ones according to a Cole–Cole plot with *W* labeled by *P* in spectrum 3, Figs. 1b, 1c. A change of charged state of *K*(*K*')-point for MWCNTs is associated with mass transfer that charged MWCNT-end states emerge. Meanwhile, the plasma oscillations of produced charged carriers shield electric fields of charged electrodes. Mass transfer for the complex ds-DNA probe/ MWCNT is observed that a dielectric spectrum of EIS-transducer including the complexes ds-DNA probe/MWCNT is characterized by presence of Warburg impedance in a Cole–Cole plot labeled by "On" in Fig. 1c.

It testifies redox activity of the ds-DNA probe on MWCNT-surface. Figure 1c shows that a dielectric band of duplex (Cole–Cole plot labeled by "DNA" in dielectric spectrum 3) appears after specific hybridization.

4. CONCLUSIONS

So, dielectric and Raman spectral analysis of DNA hybridization on surface of decorated-MWCNT

monolayer suspended on nanopores has been performed. It has been shown that self-redox activity of carboxylated MWCNTs decorated by nanocyclic organometallic complexes can be used to discriminate single-nucleotide polymorphism of colorectal tumor genome.

FUNDING

The work is supported by the grant 3.2.16 in the framework of GPSI Energetic systems, processes and technologies, the Ministry of Education and National Academy of Science, Republic of Belarus.

CONFLICT OF INTEREST

The authors declare no conflict of interest associated with this manuscript.

REFERENCES

1. E. Rasouli, Z. Shahnavaz, W. J. Basirun, et al., Anal. Biochem. **556**, 136 (2018).
2. H. Grushevskaya, N. Krylova, A. Babenka, et al., Semiconductors **52**, 1836 (2018).
3. P. A. Rasheed and N. Sandhyarani, Biosens. Bioelectron. **97**, 226 (2017).
4. H. Grushevskaya, N. Krylova, A. Babenka, et al., Int. J. Mod. Phys. B **32**, 1840033 (2018).

SPELL: OK